

RSC Advances



This is an *Accepted Manuscript*, which has been through the Royal Society of Chemistry peer review process and has been accepted for publication.

Accepted Manuscripts are published online shortly after acceptance, before technical editing, formatting and proof reading. Using this free service, authors can make their results available to the community, in citable form, before we publish the edited article. This *Accepted Manuscript* will be replaced by the edited, formatted and paginated article as soon as this is available.

You can find more information about *Accepted Manuscripts* in the [Information for Authors](#).

Please note that technical editing may introduce minor changes to the text and/or graphics, which may alter content. The journal's standard [Terms & Conditions](#) and the [Ethical guidelines](#) still apply. In no event shall the Royal Society of Chemistry be held responsible for any errors or omissions in this *Accepted Manuscript* or any consequences arising from the use of any information it contains.



Formation of Lipid and Polymer Based Gold Nanohybrids Using a Nanoreactor Approach

Dominik Witzigmann,^a Sandro Sieber,^a Fabiola Porta,^a Philip Grossen,^a Andrej Bieri,^b Natalja Strelnikova,^c Thomas Pfohl,^c Cristina Prescianotto-Baschong,^d Jörg Huwyler^{a*}

Received 00th July 20xx,
Accepted 00th July 20xx

DOI: 10.1039/x0xx00000x

www.rsc.org/

Nanocarriers encapsulating gold nanoparticles (AuNPs) hold tremendous promise for numerous biomedical applications. So far only a few fabrication strategies have been investigated and efficient processes for the manufacturing of gold nanohybrids (AuNHys) are still missing. We encapsulated a tetrachloroaurate/citrate mixture within nanocarriers and initiated the AuNP formation after self-assembly of the nanomaterial by a temperature shift. This nanoreactor approach was successfully combined with the film-rehydration, nanoprecipitation, or microfluidics method. Different nanomaterials were validated including phospholipids and copolymers and the process was optimized towards encapsulation efficiency and physico-chemical homogeneity of AuNHys. Our nanoreactor technology is versatile, efficient, and highly reproducible. Dynamic light scattering and electron microscopy techniques confirmed that generated lipid and polymer based AuNHys were of uniform size below 130 nm and contained a single AuNP. The AuNHys solutions had a deep-red color and exhibited the specific surface plasmon absorption of AuNPs. The unique optical properties of AuNHys were used to visualize cellular uptake of nanocarriers in vitro demonstrating the promising applicability of AuNHys as bioimaging tool.

Keywords: gold nanoparticle; nanoreactor; liposome; polymer nanoparticle; hybrid system; microfluidics; bioimaging

1. Introduction

Gold nanoparticles (AuNPs) have attracted great interest since Michael Faraday first described them in 1857.^{1,2} The application of AuNPs in the field of imaging and therapy were based on their unique properties, which include; (I) advantageous physico-chemical characteristics, (II) non-toxic and inert properties, (III) facile preparation of monodisperse AuNPs, and (IV) various modification options.^{3–5} Different methods for the synthesis of AuNPs have been described.^{6,7} The most widely used approach is the chemical reduction of gold salt (Au³⁺) such as tetrachloroaurate (HAuCl₄) to metallic gold (Au⁰) using the Turkevich^{8,9} or Brust-Schiffrin¹⁰ method. Moreover, synthesis methods using microwaves, UV irradiation, microfluidics, or biologic approaches were examined.^{3,11} Ultimately, AuNPs have to be modified with capping agents to avoid aggregation, provide solubility in aqueous media, and improve stability.¹²

Encapsulation of AuNPs into different nanocarriers such as liposomes or polymeric nanoparticles is an interesting option for a wide range of applications such as smart drug delivery, imaging, or photothermal therapy.^{13–18} In recent decades, great progress has been made in the field of hybrid nanocarriers using AuNPs and several strategies for their synthesis have been investigated. For example, lipid based gold nanohybrids (lipid-AuNHys) have been prepared using the following methods: improved cholerae

^a Division of Pharmaceutical Technology, Department of Pharmaceutical Sciences, University of Basel, Klingelbergstrasse 50, Basel CH-4056, Switzerland

^b Center for Cellular Imaging and NanoAnalytics (C-CINA), Biozentrum, University of Basel, Mattenstrasse 26, Basel CH-4058, Switzerland

^c Department of Chemistry, University of Basel, Klingelbergstrasse 80, Basel CH-4056, Switzerland

^d Biozentrum, University of Basel, Klingelbergstrasse 70, Basel CH-4056, Switzerland

* Author for correspondence

Electronic Supplementary Information (ESI) available: [details of any supplementary information available should be included here]. See DOI: 10.1039/x0xx00000x

dialysis¹⁹, incorporation of hydrophobic AuNPs^{20–22}, physical absorption^{23,24}, or precipitation of gold within liposomes using either, glycerol including formation or reverse-phase evaporation^{25,26}.

However, these strategies exhibited marked variability in homogeneity, reproducibility, size distribution, and morphology of gold nanohybrids (AuNHys). To overcome these challenges, we developed a novel and versatile strategy to encapsulate AuNPs into different nanocarriers with high reproducibility using a nanoreactor approach. The goal of the present study was, (I) the encapsulation of a tetrachloroaurate/citrate mixture within nanocarriers and (II) the initiation of AuNP formation after self-assembly of the nanomaterial. Selected nanomaterials (i.e. lipid and polymer based) were validated and the encapsulation efficiency, homogeneity, and robustness of our approach were optimized. Nanocarriers loaded with AuNPs were prepared by three different methods depending on the physico-chemical properties of the nanocarrier material.

The film-rehydration-extrusion method²⁷ was used for conventional (non-PEGylated) liposomes, the nanoprecipitation method²⁸ was used for di-block copolymer nanoparticles, and the microfluidics method^{29,30} was used for PEGylated (sterically stabilized) liposomes (Figure 1). The most important feature of our nanoreactor approach is the production of nanocarriers at room temperature (RT), which avoids the formation of AuNPs before self-assembly. AuNP formation is subsequently initiated by a temperature shift. The applicability of the AuNHys as bioimaging tool was demonstrated *in vitro* using HepG2 human hepatocellular carcinoma cells.

2. Experimental section

2.1 AuNP synthesis

AuNPs were synthesized following a modified Turkevich method.⁷ Optimization of AuNP synthesis using a 2³ full factorial design of experiment (DoE) [Stavex 5.2, Aicos Technologies, Basel, Switzerland] is described in detail in the Supplementary Information (Table S1). Briefly, ddH₂O with 1 mM tetrachloroaurate (Sigma-Aldrich, Buchs, Switzerland) were heated to 70°C for 20 min under vigorous stirring. To start the formation of AuNPs, citrate solution (170 mM; 50 mg mL⁻¹) was added as a reducing and capping reagent. The HAuCl₄/citrate gold reaction mixture (AuR-solution) was stirred at 70°C for 10 min until the solution had a deep-red color.

2.2 AuNHyb formation using film rehydration

The film rehydration method was used for lipids with a transition temperature (T_m) below RT with modifications described elsewhere.³¹ Liposomes were produced at a temperature which inhibits the AuNP formation. In brief, 1-palmitoyl-2-oleoyl-sn-glycero-3-phosphocholine (15 μmol) [POPC] (Avanti Polar-Lipids, Alabaster, USA) and 1-palmitoyl-2-oleoyl-sn-glycero-3-phospho-1'-rac-glycerol (5 μmol) [POPG] (Avanti Polar-Lipids, Alabaster, USA) were dissolved in chloroform/methanol (2:1, v/v) and a homogenous dry lipid film was prepared using a Rotavapor A-134 (Büchi, Flawil, Switzerland). The lipid film was rehydrated with a freshly prepared AuR-solution (HAuCl₄:citrate ratio - 1:4) at RT and 120 rpm for 10 min with 3 g glass beads (diameter 5 mm). Different lipid (20 mM) to AuR-solution ratios were tested starting from 1 mM HAuCl₄/4.1 mM citrate up to 8 mM HAuCl₄/32.8 mM citrate.

The resulting multilamellar vesicles were subjected to three freeze-thaw cycles and extruded through polycarbonate membranes with two different pore sizes using a barrel extruder (Lipex; Northern Lipids, Vancouver; Canada). Liposomes were extruded at RT 3 times through a 200 nm polycarbonate membrane and 11 times through a membrane with a pore size of 100 nm (VWR International, Dietikon, Switzerland). AuNPs, which were formed during the extrusion procedure, bind to the filter membranes. Finally, the unilamellar liposomes were heated to 70°C for 10 min to start the formation of AuNPs. To separate liposomes from free AuNPs, the sample was purified by FPLC using a Superose 6 prep column (GE Healthcare, Glattbrugg, Switzerland) eluting with 0.01 M phosphate buffered saline (PBS) containing 150 mM sodium chloride, pH 7.4 (Sigma-Aldrich, Buchs, Switzerland).

2.3 AuNHyb formation using nanoprecipitation

A nanoprecipitation method was used for the di-block copolymer polyethyleneglycol-polycaprolactone [PEG-PCL] (Sigma-Aldrich, Buchs, Switzerland). The polymer (5 mg) was dissolved in THF (50 μL) [Sigma-Aldrich, Buchs, Switzerland] under constant stirring with a magnetic bar (750 rpm). The AuR-solution (HAuCl₄:citrate ratio - 1:4) was added dropwise (one drop per five seconds). The mixture was stirred for 10 min at 750 rpm followed by 10 min on a thermomixer at 70°C and 300 rpm. Different polymer to AuR-solution ratios were tested starting from 1 mM HAuCl₄/4.1 mM citrate up to 8 mM HAuCl₄/32.8 mM citrate. To separate the PEG-PCL-AuNHys from free AuNPs, a FPLC purification step was used (see above).

2.4 Microfluidics device design and fabrication

The microfluidics device was fabricated with 0.05 mm thick polystyrene foil (GoodFellow, Huntingdon, UK) and NOA 81 (Norlan, Cranberry, USA) using standard soft-lithography techniques according to the procedure described previously.^{32,33} The microfluidics device had seven inlet channels converging to a single staggered herringbone micromixer. The rectangular cross

section had dimensions of 468 μm length, 80 μm width, and 40 μm / 200 μm height (Figure 1C). Detailed experimental procedures are given in the Supplementary Information.

2.5 Flow visualization and Computational Fluid Dynamics Simulation

Detailed experimental procedures are given in the Supplementary Information.

2.6 AuNHyb formation using microfluidics

The microfluidics method was used for lipids with a transition temperature above RT (55°C). Therefore, the AuNP formation during the liposome production was hampered due to decreased temperature. 1,2-distearoyl-sn-glycero-3-phosphocholine (DSPC) [5.75 μmol] (Avanti Polar-Lipids, Alabaster, USA), cholesterol [4 μmol] (Sigma-Aldrich, Buchs, Switzerland), and 1,2-distearoyl-sn-glycero-3-phosphoethanolamine-N-(methoxy(polyethylene glycol)-2000) (DSPE-PEG2000) [0.25 μmol] (Avanti Polar-Lipids, Alabaster, USA) were dissolved in ethanol. The microfluidics device was primed with water for the outer streams and with ethanol for the central inlet (1 $\mu\text{l s}^{-1}$) using syringe pumps.

Afterwards four different syringes were connected: (I) double-distilled water, (II) citrate solution (4.1 mM - 32.8 mM), and (III) tetrachloroaurate (HAuCl_4) solution (1 mM - 8 mM) were connected to the outer streams (always with a HAuCl_4 :citrate ratio of 1:4) and (IV) lipids in ethanol (5 mM) were connected to the central inlet. The speed was set to 4 $\mu\text{l s}^{-1}$ for syringe I, 2 $\mu\text{l s}^{-1}$ for syringe II/III and 1 $\mu\text{l s}^{-1}$ for syringe IV. The sample was collected at the outlet. Finally, the liposomes were heated to 70°C for 10 min to start the formation of AuNPs. To separate lipid-AuNHybs from free AuNPs, the sample was purified by FPLC using a Superose 6 prep column eluting with 0.01 M PBS pH 7.4.

2.7 Size analysis using dynamic light scattering

Dynamic light scattering (DLS) measurements of AuNPs and all lipid- and polymer-AuNHybs were conducted using a Delsa Nano Particle Analyzer (Beckman Coulter, Nyon, Switzerland). The laser was adjusted to 658 nm and scattered light was detected at a 165° angle. Data was converted using CONTIN particle size distribution analysis. The AuNHyb size was analyzed three times in PBS at RT.

2.8 UV-Vis and fluorescence measurements

Ultraviolet-visible (UV-Vis) absorption from 260 nm to 750 nm (step size one nm) of different samples was measured using a SpectraMax M2 (Molecular Devices, Sunnyvale, USA). Fluorescence of lipid-AuNHybs containing rhodamine labelled phospholipids (Rho-PE) [Avanti Polar-Lipids, Alabaster, USA] was analyzed by excitation at 560 nm and detection between 572 nm to 750 nm.

2.9 Transmission electron microscopy of gold nanohybrids

Size and shape of the AuNPs and AuNHybs were analyzed by transmission electron microscopy (TEM) using a CM-100 (Philips, Eindhoven, Netherlands) operating at 80 kV. Samples were prepared by deposition onto a 400-mesh carbon-coated copper grid (Polysciences Inc., Eppelheim, Germany). Prior to sample deposition, the grid was exposed to plasma for 10 seconds to increase sample binding. Grids were washed with double-distilled water to prevent precipitation of uranyl salts by phosphate ions. Then the samples were negatively stained using a 2% uranylacetate solution (Sigma-Aldrich, Buchs, Switzerland), the excess of uranylacetate was removed using filter paper, and the samples were dried at RT overnight. Nanocarrier integrity was preserved by this procedure as confirmed by Cryo-EM analysis using sample vitrification (see below). To characterize the size of AuNPs inside of AuNHybs, the diameter of at least 100 AuNPs was determined.

2.10 Cryo-TEM of gold nanohybrids

Aliquots (4 μL) of AuNHybs were adsorbed onto holey-carbon supported grids (Quantifoil, Gossloebichau, Germany), blotted with Whatman 1 filter papers, and vitrified in liquid nitrogen-cooled liquid ethane using a Vitrobot IV (FEI Company, Eindhoven, Netherlands). Cryo-electron imaging was performed with a Philips CM200-FEG electron microscope operated at an acceleration voltage of 200 kV. Micrographs were recorded with a 4k \times 4k TemCam-F416 CMOS camera (TVIPS, Gauting, Germany).

2.11 Preparation of fluorescent lipid based AuNHybs

Detailed experimental procedures are given in the Supplementary Information.

2.12 Passive uptake of AuNPs and AuNHybs in HepG2 cells

HepG2 cells were seeded on a 10 cm plate and cultured in 10 mL Dulbecco's modified Eagle's culture medium high glucose supplemented with 10% fetal calf serum (FCS), 100 units mL⁻¹ penicillin, and 100 µg mL⁻¹ of streptomycin (DMEM comp). All cell culture media components were purchased from Sigma-Aldrich (Buchs, Switzerland). Cells were allowed to adhere for 24 h before the AuNPs or AuNHys were added. After incubation at 37°C for 18 h, the tissue culture plate was washed three times with DMEM comp (37°C). Afterwards, the cells were fixed with DMEM containing 3% formaldehyde (Sigma-Aldrich, Buchs, Switzerland) and 0.3% glutaraldehyde (Sigma-Aldrich, Buchs, Switzerland) for two hours at RT and stored overnight at 4°C. The following day, cells were scraped, pelleted, and washed three times with water, and then incubated with 2% uranylacetate for two hours at 4°C in the dark. The sample was washed, dehydrated by series of methanol, and infiltrated with LR-gold resin (London Resin, London, UK) according to the manufacturer's instructions. Polymerization was performed at -10°C by UV light for one day. Sections of about 70 nm were collected on carbon-coated Formavar-Ni-grids (EMS, Hatfield, USA) and stained for 15 min with 4% uranylacetate followed by two minutes in Reynolds lead citrate solution. Sections were viewed using a Phillips CM-100 electron microscope.

3. Results and discussion

3.1 Film Rehydration (Conventional Liposomes)

For the preparation of AuNP loaded liposomes, the most direct approach is the rehydration of a lipid film with presynthesized AuNPs. The well-characterized method developed by Turkevich and Frens is ideal to synthesize AuNPs with diameters of approximately 20 nm (see Supplementary Information for experimental details).^{7,34,35} However, the AuNP encapsulation approach has several issues. The AuNPs often form aggregates up to several hundred nanometers (Figure 2A), which results in low encapsulation efficiency (Figure 2D) and renders extrusion impossible due to blocked filter membranes. Therefore, we developed an alternative strategy and combined the film-rehydration method with a 'nanoreactor approach'. We rehydrated the lipid film with the Turkevich reaction mixture consisting of tetrachloroaurate and citrate. Then the formation of AuNPs was initiated inside the core of preassembled liposomes by a shift in temperature [70°C, 10 min] (Figure 1A).

To prevent the formation of AuNPs during the preparation of liposomes, we selected lipids that are characterized by a low transition temperature (T_m). The lipid composition consisted of POPC and POPG, which provides a T_m of -2°C. The lipid film was rehydrated with a tetrachloroaurate and citrate reaction solution in different ratios and the liposomes were extruded at RT before initiation of AuNP formation. The final AuNHyb sample exhibited the characteristic ruby-red color resulting from the surface plasmon resonance of encapsulated AuNPs.³⁶ To test if the temperature affected the efficiency of the process, the entire procedure was also carried out at 4°C. However, there was no difference between AuNHybs prepared at RT or at lower temperatures. TEM showed that the AuNPs were encapsulated inside the AuNHybs (Figure 2B). Encapsulation efficiency (i.e. the ratio between liposomes encapsulating AuNPs and liposomes that were empty) was significantly higher using the nanoreactor approach compared with either extrusion at high temperature (data not shown) or use of preformed AuNPs (Figure 2D). The latter condition led to the formation of AuNP aggregates in the medium surrounding the liposomes (Figure 2D). In contrast, the nanoreactor approach resulted in the encapsulation of a single AuNP in the inner liposomal core.

POPC/POPG-AuNHybs were also analyzed by Cryo-TEM (Figure 2C). Under these conditions, the native, hydrated state of the lipid formulation is presented.³⁷ Cryo-TEM showed that lipid-AuNHybs were spherical, mainly unilamellar, and efficiently loaded with AuNPs (Figure 2C). AuNPs were located in the hydrophilic core of the liposomes (Figure 2C), consistent with TEM analysis (Figure 2B). Interestingly, some AuNPs were located in close proximity to the lipid bilayer. This could be either an artefact from the drying process during the TEM grid preparation or an interaction of the AuNPs with one of the phospholipids. The number of AuNPs encapsulated was dependent on the concentration of the AuR-solution. The highest AuNP encapsulation efficiency was achieved with 4 mM tetrachloroaurate, 16.3 mM citrate, and 20 mM lipids. Higher AuR-solution to lipid ratios resulted in the formation of AuNP agglomerates outside of the liposomes. On the other hand, lower AuR-solution to lipid ratios led to a significant amount of empty nanocarriers. Interestingly, TEM analysis revealed that the AuNPs, which were synthesized inside liposomes were significantly smaller than AuNPs synthesized without lipids (approximately 12.0 nm vs. 21.5 nm) (Figure 2A vs. Figure 2B). It is tempting to speculate that the limited amount of tetrachloroaurate and citrate available inside the nanocarriers is limiting the maximum size of the AuNPs. The POPC/POPG-AuNHybs were analyzed by DLS. The size of POPC/POPG-AuNHybs (104.7 nm \pm 5.2 nm) was similar to the size of empty liposomes (Figure 3A). Thus, AuNPs did not influence the nanocarrier diameter. In Figure 4A, the absorption spectra of empty POPC/POPG liposomes (negative control), AuNPs (positive control), and POPC/POPG-AuNHybs are compared. As expected no absorption maximum was observed for empty POPC/POPG liposomes in the wavelength range from 500 nm to 600 nm. In contrast, AuNPs and POPC/POPG-AuNHybs showed a distinct surface plasmon absorbance peak at 525 nm. This indicates the successful encapsulation of AuNPs inside POPC/POPG liposomes.

3.2 Nanoprecipitation (Di-block Copolymer Nanoparticles)

To demonstrate the broad applicability of our nanoreactor approach, we investigated the formation of polymer-AuNHybs using nanoprecipitation (Figure 1B). For this method, the AuR-solution was added dropwise to the di-block copolymer PEG-PCL dissolved in THF (see Supplementary Information for experimental details). Similar to the lipid-AuNHybs, the addition of preformed AuNPs to the polymer resulted in low encapsulation efficiency (Figure S1A). In contrast, high encapsulation efficiency with one AuNP per polymeric nanocarrier was achieved using the nanoreactor approach (Figure 2E). Cryo-TEM analysis confirmed that AuNPs with a size of 14.1 nm \pm 3.1 nm were located inside the polymer-AuNHybs (Figure S1B).

Polymer-AuNHybs consisting of PEG-PCL presented a spherical morphology in which polymer chains self-assemble as solid polymeric nanoparticles. Thus, the hydrophilic parts of the di-block copolymer are exposed towards the outer buffer environment (Figure S1B). Recently, this was also shown for other polymeric nanoparticles.³⁸ DLS analysis showed monodisperse formulation of polymer-AuNHybs (polydispersity index = 0.088) with a diameter of 77.5 nm \pm 3.9 nm (Figure 3B). Additionally, the polymer-AuNHybs showed a characteristic surface plasmon band at 527 nm due to the unique optical properties of AuNPs (Figure 4B).

3.3 Microfluidics (PEGylated Liposomes)

Recently, it has been demonstrated that rapid microfluidic mixing offers a controlled method to produce lipid nanocarriers. Defined interfacial forces between the nanomaterial components result in a controllable and highly reproducible self-assembly process.⁴⁰ To facilitate the production of AuNP loaded PEGylated liposomes, we developed a microfluidics platform for the preparation of lipid-AuNHys using lipids with a transition temperature above RT. Briefly, PEGylated lipid based gold nanohybrids (PEG-Lipo-AuNHys) were synthesized by rapid mixing of an ethanolic lipid solution (5 mM, consisting of DSPC, cholesterol, and DSPE-PEG2000) and the aqueous Turkevich AuR-solution. In the last step of the process, the PEGylated liposomes were heated to 70°C to start the formation of the AuNPs inside the liposomes.

In more detail, our microfluidics device consisted of seven inlet channels which converged into a single staggered-herringbone micromixer (see Supplementary Information). At the junction of the inlets, the center stream was hydrodynamically focused to improve the mixing. To illustrate the nanomanufacturing process, we simulated the flow patterns and visualized them with a fluorescent dye (Figure 1D/E; Suppl. Figure S2). Liposomes are formed at the interface between the hydrodynamically focused lipid stream and the AuR-solution. The mechanism of controlled, focused, and rapid mixing⁴¹ is visible both in the experimental setting (Figure 1D) and the computer simulation (Figure 1E). The central inlet was used for the model ethanolic lipid solution [5mM] (Figure S2B). The other six, outer inlets were used for tetrachloroaurate (Figure S2C), citrate (Figure S2D), and water (two inlets for each solution). Syringe pumps were used with flow rates up to 4 $\mu\text{L s}^{-1}$. The reagents were supplied by separate inlets because the use of tetrachloroaurate and citrate in the same inlet resulted in premature AuNP formation in the herringbone micromixer (Figure S3D).⁴⁰ In addition, the use of preformed AuNPs resulted in a low encapsulation efficiency, as observed for the film-rehydration and nanoprecipitation method with preformed AuNPs (Figure S3E). Therefore, the best results were achieved using a microfluidics platform with seven different inlets (Figure 1C-E).

Water (4 $\mu\text{L s}^{-1}$) was used to improve the hydrodynamic flow focusing of the lipid stream and to decrease the final ethanol concentration. Furthermore, we used a higher flow rate for the outer inlets to increase the water to ethanol ratio. This is important to prevent the destabilization of liposomes caused by elevated ethanol concentrations.⁴² Microfluidics parameters were adjusted to optimize encapsulation efficiency and size distribution. A continuous and efficient production was achieved with 2 mM tetrachloroaurate / 8.2 mM citrate solution (for 5 mM lipids); and flow rates of 2 $\mu\text{L s}^{-1}$ for the AuR-solutions, and 1 $\mu\text{L s}^{-1}$ for the lipid solution. The absolute production speed was 420 $\mu\text{L min}^{-1}$ (Figure S2A). Increasing the concentration of the AuR-solution for the microfluidics manufacturing resulted in an increased number of encapsulated AuNPs per AuNHyp (Figure S3A-C) until agglomerates were observed. AuNHys with several encapsulated AuNPs mostly resulted in Janus-like vesicle structures (i.e. asymmetrical loading) as recently shown for Janus magnetic liposomes.⁴³ DLS and TEM showed that the size of PEG-Lipo-AuNHys was similar to that of empty PEGylated liposomes (Figure 2F; Figure 3C). PEG-Lipo-AuNHys with a mean hydrodynamic diameter of 123 nm \pm 2.5 nm (Z-average) and a monodisperse size distribution were obtained (Figure 3C). Each liposome incorporated one AuNP with a diameter of 6.8 nm \pm 1.5 nm as shown by TEM (Figure 2F). A characteristic plasmon absorption at 525 nm was observed using UV-Vis spectroscopy (Figure 4C).

3.4 Characterization of Nanoreactor Approach

We showed that our nanoreactor approach is applicable for a wide range of nanomaterials, as well as different preparation methods. The film rehydration method can be used for lipids with a transition temperature below RT, whereas the nanoprecipitation method is suitable for several polymer nanomaterials.^{28,44} The microfluidics method is especially designed for lipids with a transition temperature above RT. However, this technique is suitable for all nanomaterials, that need highly controlled nanomanufacturing.⁴⁰

The most important step of our nanoreactor approach is the speed of the nanocarrier production. The nanocarrier formation needs to be faster than AuNP aggregate formation. Therefore, the AuNP formation inside the nanocarriers is initiated by a temperature shift after self-assembly. AuNP aggregates formed outside of the self-assembled nanocarrier are removed by size exclusion chromatography. During this step, the outer buffer can be exchanged to a physiological compatible medium such as PBS. Several publications have shown that a difference in tonicity between the nanocarrier lumen and the outer buffer environment is not affecting the stability or morphology of nanocarriers.⁴⁵⁻⁴⁷

All tested combinations resulted in efficient and reproducible formation of AuNHys. Moreover, DLS, TEM, and Cryo-TEM analysis showed that the final AuNHys preserved the initial dimensions of the empty nanocarriers. Four distinct observations indicate that the AuNPs were encapsulated inside the nanocarriers. Firstly, the AuNHys passed easily through the size exclusion chromatography medium (Superose 6 prep) whereas non-encapsulated AuNPs showed a high affinity for the chromatography medium, which was recently also shown for quantum dots.⁴⁸ Secondly, the AuNHys exhibited an improved stability in PBS and aggregation was prevented as compared to free AuNPs. Thirdly, electron microscopy analysis showed a single AuNP entrapped per nanocarrier and no clusters of AuNPs were observed. Finally, the deep-red AuNHyp solutions exhibited a specific surface plasmon absorption peak at 525 nm, and a low 650 nm/530 nm ratio, which is characteristic for non-agglomerated AuNPs.⁴⁹

3.5 Cellular Uptake Experiments

To demonstrate the use of AuNHybs for bioimaging, we performed uptake experiments with the AuNHybs in HepG2 cells exploiting the unique optical properties of AuNPs. The electron-density of AuNPs was used for further TEM analysis of cells (Figure 5) as shown recently for surface-modified AuNPs.⁵⁰ Due to the high quality and uniform size of AuNPs, TEM observations were possible without silver enhancement. Using this approach, fundamental insights about nanocarrier uptake and intracellular fate can be obtained. For example, proteins covering the surface of nanocarriers after administration to biological medium can influence cellular uptake. However, formation of a protein corona and opsonisation can be minimized using PEGylated nanocarriers (i.e. PEG-PCL nanoparticles or PEGylated liposomes).^{51,52} It remains to be elucidated to which degree protein adsorption onto non-modified nanocarriers such as conventional liposomes has to be taken into account for biomedical applications.^{53,54}

The interaction of free AuNPs with HepG2 cells is shown in Figure 5A and 5D. Free AuNPs formed aggregates which were located on the cellular plasma membrane (Figure 5A) or taken up into the cell (Figure 5D). These observations are in agreement with published results.^{50,55} Figure 5 shows the interaction with cells of lipid (Panel B/E) or polymer based AuNHybs (Panel C/F). In contrast to the uptake of free AuNPs, no AuNP aggregates were detected using AuNHybs. Different internalization steps were observed. An early stage in the cellular uptake mechanism was indicated by parts of the cellular plasma membrane around endosomes located near the cellular membrane (Figure 5B). Compartments filled with more than one AuNP are most likely caused during maturation of different AuNHyb-filled vesicles (Figure 5E/F).

AuNHybs could thus be used to examine nanoparticle-cell-interactions and the intracellular fate of the nanocarriers inside the cells using TEM, a technique which offers greater resolution compared to confocal microscopy. It should be noted that liposomes encapsulating AuNPs can act simultaneously as a carrier for fluorescent dyes (see Supplementary Information for experimental details). For example rhodamine labelled phospholipids (Rho-PE) can be used to fluorescence label AuNHybs (Figure S4b). This offers the possibility to image fluorescent AuNHybs by confocal fluorescence microscopy or to quantify them with flow cytometry analysis.

4. Conclusions

In conclusion, we have developed a novel strategy for the preparation of lipid and polymer based AuNHybs. After encapsulation of the required reagents inside nanocarriers, formation of AuNPs was triggered by a temperature shift. In future, a similar approach could be used for the preparation of alternative metal nanohybrids such as silver nanoparticles. Different preparation techniques were used in combination with various nanomaterials. To the best of our knowledge, this nanoreactor approach is unique and was not used previously. The high reproducibility and versatility of our nanoreactor approach is unprecedented and makes this technology suitable for many nanomaterials. Microfluidics offers the possibility for an efficient and large scale production.

The produced AuNHybs have a size of 70 nm to 130 nm, which makes them ideal for bioimaging applications⁵⁶. In addition, AuNHybs can be stored over a prolonged period of time (i.e. >3 months / 4°C) maintaining their initial size and monodispersity. In order to target specific cells or tissues, AuNHybs can be easily modified using surface-conjugated receptor ligands⁵⁷. Our nanoreactor approach will be instrumental to develop a better understanding of cellular uptake and intracellular trafficking of targeted nanocarriers.

Acknowledgements

The authors declare no conflicting financial interest. Funding of the Stiftung zur Förderung des pharmazeutischen Nachwuchses in Basel is acknowledged. C.P.-B. was supported by the Swiss National Science Foundation (31003A-125423). D.W. thanks Lisa Stoltenburg for her support during this project. The authors thank Dr. Adam Lister for editorial and Andrea Fehrenbach for graphical assistance. In addition, we thank Dr. Susanne H. Schenk for her feedback on the manuscript, Dr. Timothy Sharpe for his scientific input, and Prof. Henning Stahlberg (Director of C-CINA, Centre for Cellular Imaging and NanoAnalytics) and the Microscopy Center of the Biozentrum Basel for their support with electron microscopy techniques.

Notes and references

- 1 A. S. Thakor, J. Jokerst, C. Zavaleta, T. F. Massoud and S. S. Gambhir, *Nano Lett.*, 2011, **11**, 4029–4036.
- 2 D. F. Moyano, B. Duncan and V. M. Rotello, *Methods Mol. Biol.*, 2013, **1025**, 3–8.
- 3 D. Kumar, N. Saini, N. Jain, R. Sareen and V. Pandit, *Expert Opin. Drug Delivery*, 2013, **10**, 397–409.
- 4 R. Cao-Milán and L. M. Liz-Marzán, *Expert Opin. Drug Delivery*, 2014, **11**, 741–752.
- 5 L. C. Kennedy, L. R. Bickford, N. A. Lewinski, A. J. Coughlin, Y. Hu, E. S. Day, J. L. West and R. A. Drezek, *Small*, 2011, **7**, 169–183.
- 6 E. Oh, K. Susumu, R. Goswami and H. Mattoussi, *Langmuir*, 2010, **26**, 7604–7613.
- 7 C. Li, D. Li, G. Wan, J. Xu and W. Hou, *Nanoscale Res. Lett.*, 2011, **6**, 440.
- 8 S. K. Sivaraman, S. Kumar and V. Santhanam, *J. Colloid Interface Sci.*, 2011, **361**, 543–547.
- 9 J. Kimling, M. Maier, B. Okenve, V. Kotaidis, H. Ballot and A. Plech, *J. Phys. Chem. B*, 2006, **110**, 15700–15707.
- 10 P. J. G. Goulet and R. B. Lennox, *J. Am. Chem. Soc.*, 2010, **132**, 9582–9584.
- 11 L. L. Lazarus, A. S.-J. Yang, S. Chu, R. L. Brutchey and N. Malmstadt, *Lab Chip*, 2010, **10**, 3377–3379.
- 12 W. Wang, Q.-Q. Wei, J. Wang, B.-C. Wang, S. Zhang and Z. Yuan, *J. Colloid Interface Sci.*, 2013, **404**, 223–229.
- 13 D. Pornpattananangkul, S. Olson, S. Aryal, M. Sartor, C.-M. Huang, K. Vecchio and L. Zhang, *ACS Nano*, 2010, **4**, 1935–1942.
- 14 D. V. Volodkin, A. G. Skirtach and H. Möhwald, *Angew. Chem., Int. Ed. Engl.*, 2009, **48**, 1807–1809.
- 15 M. R. Preiss and G. D. Bothun, *Expert Opin. Drug Delivery*, 2011, **8**, 1025–1040.
- 16 A. K. Rengan, M. Jagtap, A. De, R. Banerjee and R. Srivastava, *Nanoscale*, 2014, **6**, 916–923.
- 17 G. Von White, Y. Chen, J. Roder-Hanna, G. D. Bothun and C. L. Kitchens, *ACS Nano*, 2012, **6**, 4678–4685.
- 18 J. Nam, Y. S. Ha, S. Hwang, W. Lee, J. Song, J. Yoo and S. Kim, *Nanoscale*, 2013, **5**, 10175–10178.
- 19 H. Minematsu, T. Otani, T. Oohashi, M. Hirai, K. Oie, K. Igarashi and A. Ohtsuka, *J. Electron Microsc.*, 2011, **60**, 95–99.
- 20 M. R. Rasch, E. Rossinyol, J. L. Hueso, B. W. Goodfellow, J. Arbiol and B. A. Korgel, *Nano Lett.*, 2010, **10**, 3733–3739.
- 21 S.-H. Park, S.-G. Oh, J.-Y. Mun and S.-S. Han, *Colloids Surf., B*, 2006, **48**, 112–118.
- 22 L. Paasonen, T. Sipilä, A. Subrizi, P. Laurinmäki, S. J. Butcher, M. Rappolt, A. Yaghmur, A. Urtti and M. Yliperttula, *J. Controlled Release*, 2010, **147**, 136–143.
- 23 C. Kojima, Y. Hirano, E. Yuba, A. Harada and K. Kono, *Colloids Surf., B*, 2008, **66**, 246–252.
- 24 T. K. Sau, A. S. Urban, S. K. Dondapati, M. Fedoruk, M. R. Horton, A. L. Rogach, F. D. Stefani, J. O. Rädler and J. Feldmann, *Colloids Surf., A*, 2009, **342**, 92–96.
- 25 R. Genç, G. Clergeaud, M. Ortiz and C. K. O'Sullivan, *Langmuir*, 2011, **27**, 10894–10900.
- 26 K. Hong, D. S. Friend, C. G. Glabe and D. Papahadjopoulos, *Biochim. Biophys. Acta*, 1983, **732**, 320–323.
- 27 J. Huwyler, D. Wu and W. M. Pardridge, *Proc. Natl. Acad. Sci. U. S. A.*, 1996, **93**, 14164–14169.
- 28 T. Govender, S. Stolnik, M. C. Garnett, L. Illum and S. S. Davis, *J. Controlled Release*, 1999, **57**, 171–185.
- 29 Y. Kim, B. Lee Chung, M. Ma, W. J. M. Mulder, Z. A. Fayad, O. C. Farokhzad and R. Langer, *Nano Lett.*, 2012, **12**, 3587–3591.
- 30 L. Y. Yeo, H.-C. Chang, P. P. Y. Chan and J. R. Friend, *Small*, 2011, **7**, 12–48.
- 31 P. Detampel, D. Witzigmann, S. Krähenbühl and J. Huwyler, *J. Drug Targeting*, 2013, **22**, 232–241.
- 32 S. Deshpande and T. Pfohl, *Biomicrofluidics*, 2012, **6**, 34120.
- 33 M. E. Brennich, J.-F. Nolting, C. Dammann, B. Nöding, S. Bauch, H. Herrmann, T. Pfohl and S. Köster, *Lab Chip*, 2011, **11**, 708–716.
- 34 J. Turkevich, P. C. Stevenson and J. Hillier, *Discuss. Faraday Soc.*, 1951, **11**, 55–75.
- 35 G. Frens, *Nature-Physical Science*, 1973, **241**, 20–22.
- 36 E. Casals, T. Pfaller, A. Duschl, G. J. Oostingh and V. Puntès, *ACS Nano*, 2010, **4**, 3623–3632.
- 37 S. Mornet, O. Lambert, E. Duguet and A. Brisson, *Nano Lett.*, 2005, **5**, 281–285.
- 38 E. Jäger, A. Jäger, T. Etrych, F. C. Giacomelli, P. Chytil, A. Jigounov, J.-L. Putaux, B. Říhová, K. Ulbrich and P. Štěpánek, *Soft Matter*, 2012, **8**, 9563–9575.

- 39 I. V. Zhigaltsev, N. Belliveau, I. Hafez, A. K. K. Leung, J. Huft, C. Hansen and P. R. Cullis, *Langmuir*, 2012, **28**, 3633–3640.
- 40 A. Jahn, W. N. Vreeland, M. Gaitan and L. E. Locascio, *J. Am. Chem. Soc.*, 2004, **126**, 2674–2675.
- 41 P. M. Valencia, P. A. Basto, L. Zhang, M. Rhee, R. Langer, O. C. Farokhzad and R. Karnik, *ACS Nano*, 2010, **4**, 1671–1679.
- 42 N. Maurer, K. F. Wong, H. Stark, L. Louie, D. McIntosh, T. Wong, P. Scherrer, S. C. Semple and P. R. Cullis, *Biophys. J.*, 2001, **80**, 2310–2326.
- 43 C. Bonnaud, C. A. Monnier, D. Demurtas, C. Jud, D. Vanhecke, X. Montet, R. Hovius, M. Lattuada, B. Rothen-Rutishauser and A. Petri-Fink, *ACS Nano*, 2014, **8**, 3451–3460.
- 44 U. Bilati, E. Allémann and E. Doelker, *Eur. J. Pharm. Sci.*, 2005, **24**, 67–75.
- 45 D. D. Lasic, B. Ceh, M. C. Stuart, L. Guo, P. M. Frederik and Y. Barenholz, *Biochim. Biophys. Acta*, 1995, **1239**, 145–156.
- 46 null Ceh and null Lasic, *J Colloid Interface Sci*, 1997, **185**, 9–18.
- 47 A. Fritze, F. Hens, A. Kimpfler, R. Schubert and R. Peschka-Süss, *Biochim. Biophys. Acta, Biomembr.*, 2006, **1758**, 1633–1640.
- 48 M. Camblin, P. Detampel, H. Kettiger, D. Wu, V. Balasubramanian and J. Huwyler, *Int. J. Nanomed.*, 2014, **9**, 2287–2298.
- 49 C.-C. Huang, Y.-F. Huang, Z. Cao, W. Tan and H.-T. Chang, *Anal. Chem.*, 2005, **77**, 5735–5741.
- 50 P. Nativo, I. A. Prior and M. Brust, *ACS Nano*, 2008, **2**, 1639–1644.
- 51 D. Pozzi, V. Colapicchioni, G. Caracciolo, S. Piovesana, A. L. Capriotti, S. Palchetti, S. D. Grossi, A. Riccioli, H. Amenitsch and A. Laganà, *Nanoscale*, 2014, **6**, 2782–2792.
- 52 M. Lundqvist, J. Stigler, T. Cedervall, T. Berggård, M. B. Flanagan, I. Lynch, G. Elia and K. Dawson, *ACS Nano*, 2011, **5**, 7503–7509.
- 53 M. Lundqvist, J. Stigler, G. Elia, I. Lynch, T. Cedervall and K. A. Dawson, *PNAS*, 2008, **105**, 14265–14270.
- 54 M. Hadjidemetriou, Z. Al-Ahmady, M. Mazza, R. F. Collins, K. Dawson and K. Kostarelos, *ACS Nano*, 2015.
- 55 B. D. Chithrani, A. A. Ghazani and W. C. W. Chan, *Nano Lett.*, 2006, **6**, 662–668.
- 56 H. Kettiger, A. Schipanski, P. Wick and J. Huwyler, *Int. J. Nanomed.*, 2013, **8**, 3255–3269.
- 57 A. Wicki, D. Witzigmann, V. Balasubramanian and J. Huwyler, *J. Controlled Release*, 2015, **200**, 138–157.

Figures

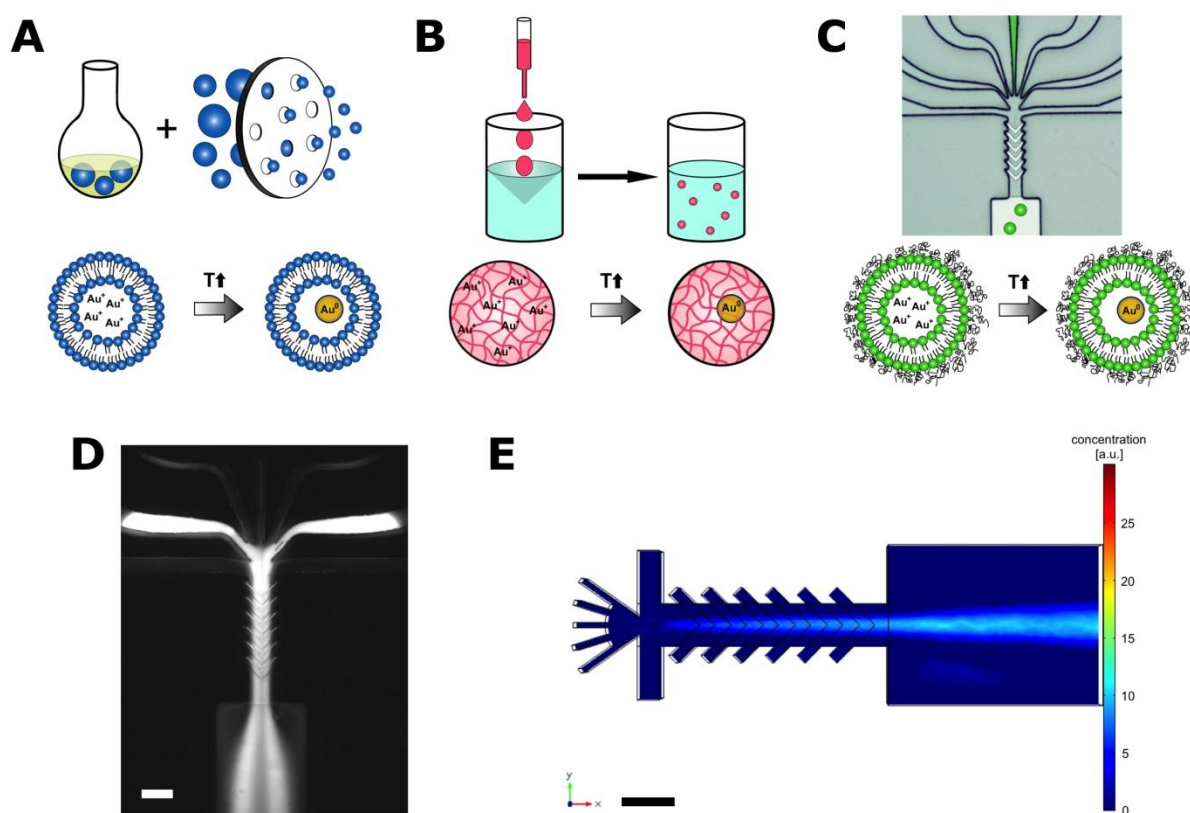


Figure 1. Different methods for the preparation of gold nanohybrids. Schematic representation of the, (A) film-rehydration-extrusion method for lipids with $T_m < \text{room temperature (RT)}$, (B) nanoprecipitation method for the di-block copolymer PEG-PCL, and (C) microfluidics platform for lipids with $T_m > \text{RT}$. The formation of gold nanoparticles inside the nanocarriers was initiated by temperature increase after self-assembly. (C) The microfluidics device had seven inlet channels converging to a single staggered herringbone micromixer. (D) Microfluidic streams were visualized using the fluorescence dye fluorescein. (E) Computational fluid dynamics simulation of concentration gradients (in a.u.) in the microfluidics device. Scale bars indicate 100 μm .

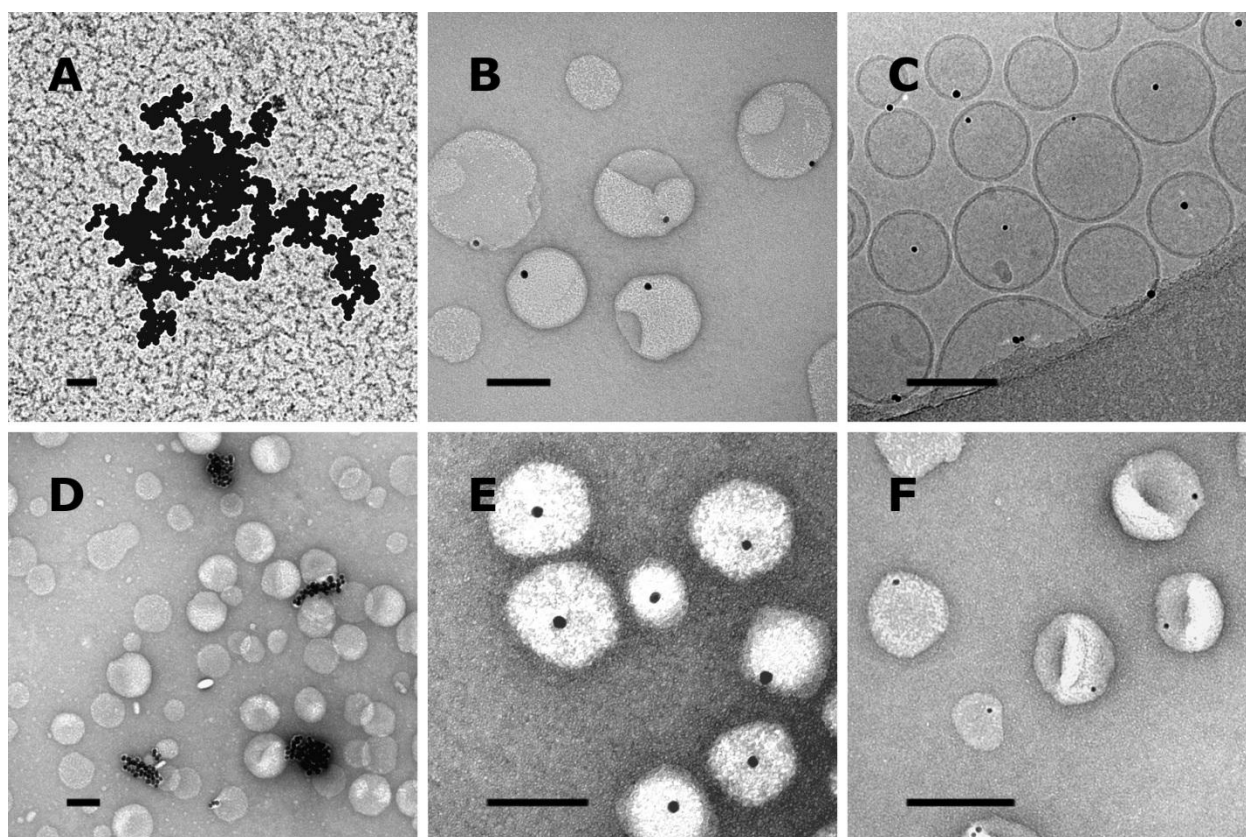


Figure 2. Characterization of gold nanoparticles (AuNPs) and gold nanohybrids (AuNHybs). Representative transmission electron microscopy (TEM) (A/B, D-F) and Cryo-TEM (C) images are shown. (A) AuNPs were synthesized using a modified Turkevich method. (B) POPC/POPG-AuNHybs were analyzed by TEM and (C) Cryo-TEM. (D) The film-rehydration method for a lipid formulation with preformed AuNPs resulted in agglomerates. (E) PEG-PCL-AuNHybs prepared by nanoprecipitation and (F) PEG-liposome-AuNHybs after microfluidics platform preparation contain a single AuNP. Scale bars indicate 100 nm.

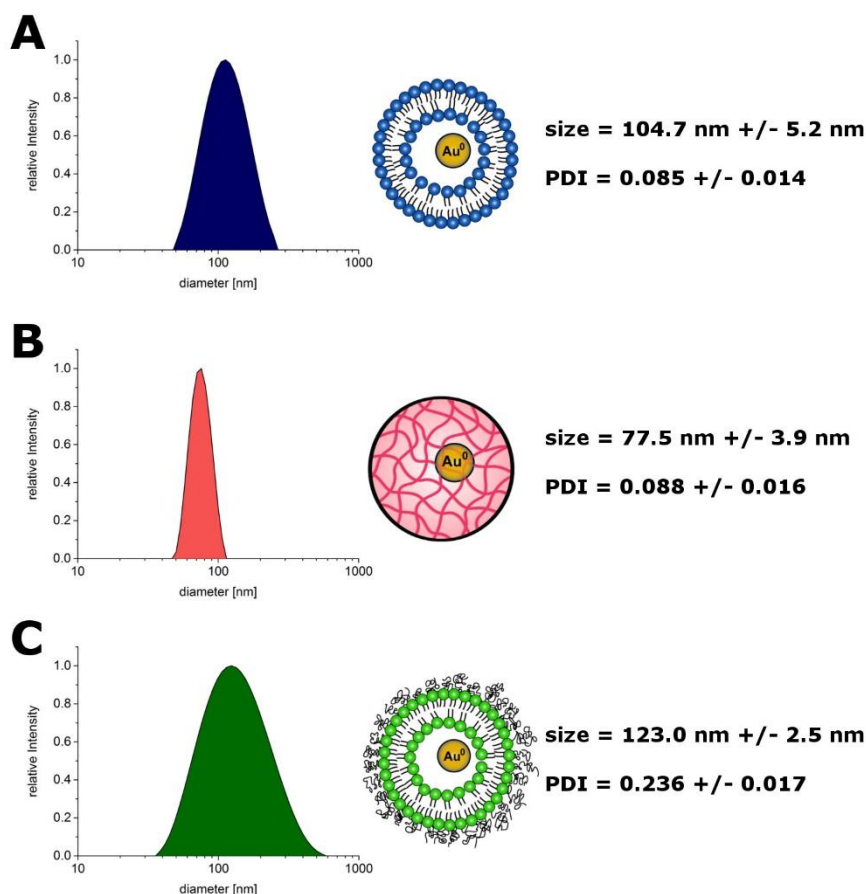


Figure 3. Dynamic light scattering analysis of gold nano hybrids (AuNHybs). Intensity distribution of (A) POPC/POPG-AuNHyb, (B) PEG-PCL-AuNHyb, and (C) PEGylated liposome-AuNHyb. Mean values of size and polydispersity index (PDI) are given \pm SD (n=5).

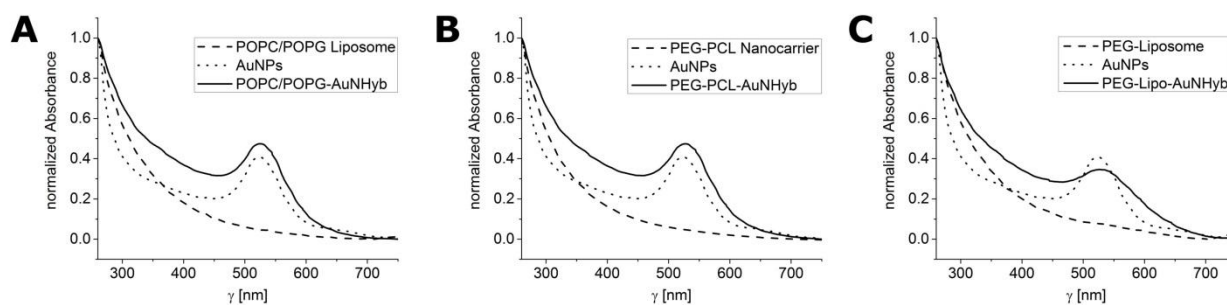


Figure 4. UV spectra of empty nanocarriers, gold nanoparticles (AuNPs), and gold nano hybrids (AuNHybs). Relative UV-Vis absorption from 260 nm to 750 nm (step size one nm) was measured for (A) POPC/POPG, (B) PEG-PCL, and (C) PEG-lipid based nanocarriers. Spectra were normalized to an OD₂₆₀ of 1.0. All AuNHybs showed a characteristic surface plasmon band at approximately 525 nm.

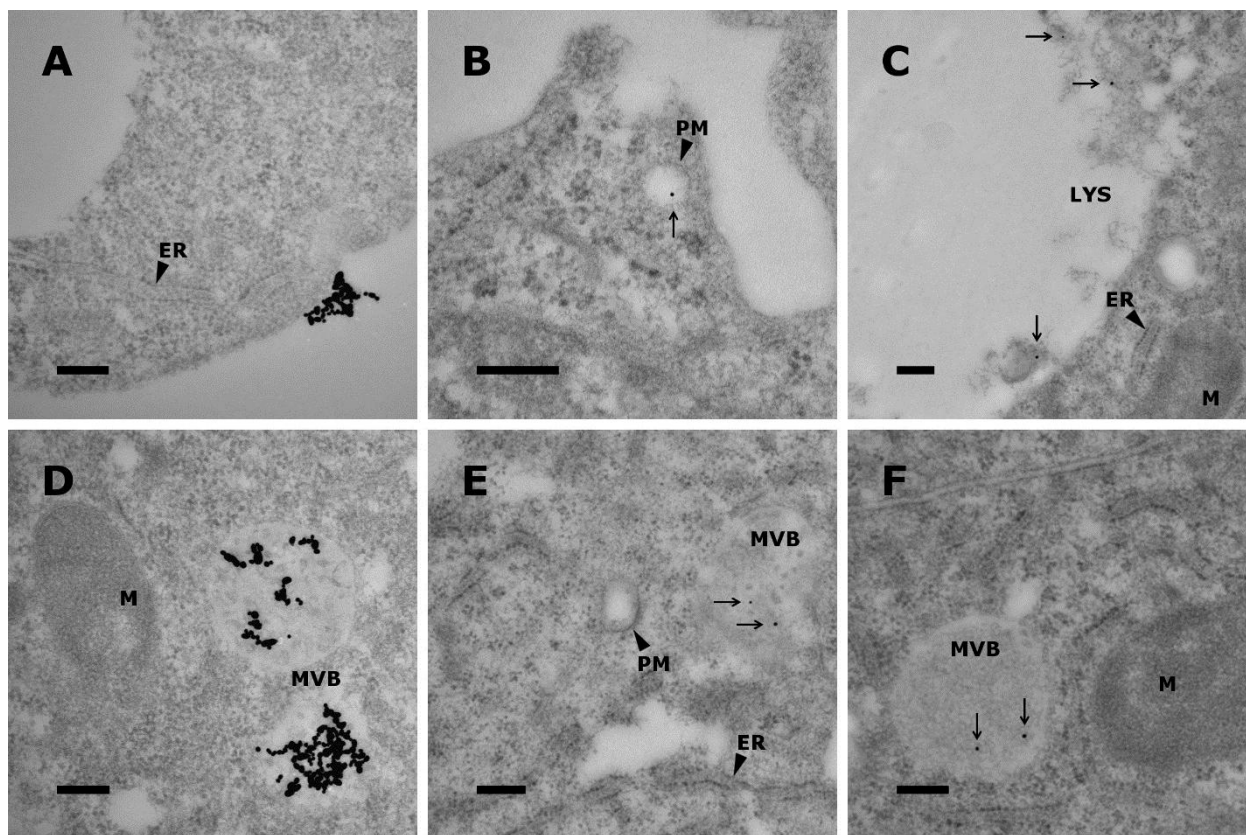


Figure 5. Uptake experiments of gold nanoparticles (AuNPs) and gold nanohybrids (AuNHys) in HepG2 cells. (A) AuNPs localized at the cell surface or (D) inside the cell. Representative uptake images of (B/E) POPC/POPG-AuNHys and (C/F), PEG-PCL-AuNHys (Arrows). ER = endoplasmic reticulum; LYS = Lysosome; M = mitochondria; MVB = multi vesicular body; PM = plasma membrane. Scale bars indicate 200 nm.

Table of contents

Formation of Lipid and Polymer Based Gold Nanohybrids Using a Nanoreactor Approach

Dominik Witzigmann, Sandro Sieber, Fabiola Porta, Philip Grossen, Andrej Bieri, Natalja Strelnikova, Thomas Pfohl, Cristina Precianotto-Baschong, Jörg Huwyler *

Nanocarriers encapsulating gold nanoparticles hold tremendous promise for biomedical applications. The nanoreactor approach offers a versatile, efficient, and highly reproducible preparation technology.

